National Transportation Safety Board
Office of Research and Engineering
Washington, DC 20594

DCA22FA132

MATERIALS LABORATORY

Specialist's Factual Report 22-085

December 7, 2022

(This page intentionally left blank)

A. ACCIDENT INFORMATION

Location: Miami, Florida
Date: June 21, 2022
Time: 17:38 eastern daylight time
21:38 coordinated universal time
Vehicle: McDonnell Douglas MD-82, HI1064
Investigator: Steve Magladry, AS-40

B. COMPONENTS EXAMINED

Remnant of a shimmy damper lockwire
Belleville washer

C. EXAMINATION PARTICIPANTS

Specialist Erik Mueller, Ph.D., P.E.
Office of Research and Engineering, NTSB
Washington, DC

D. DETAILS OF THE EXAMINATION

On June 21, 2022, RED Air flight 203, a Boeing MD-82, experienced a left main landing gear failure shortly after landing at Miami International Airport (MIA), Miami, Florida. The airplane departed the runway, and a post-crash fire occurred. The airplane was evacuated, with four passengers receiving minor injuries. The flight officer stated that during the landing, the crew felt a vibration on the left side followed by the left main gear collapsing. The aircraft wreckage was documented and moved to a secure location during the on-scene portion of the investigation. The left and right main landing gears were removed from the aircraft for further evaluation, and several small components were sent to the NTSB Materials Laboratory for additional examination.

One of the components from the accident airplane was a Belleville washer (Figure 1). The washer exhibited a through-thickness radial crack located in the 12 o'clock position, as shown in Figure 1. The washer was measured with digital calipers. The inner diameter was 2.352 inches, and the outer diameter was 3.140 inches. The radial width was 0.392 inches, and the thickness was measured as 0.083 inches.

Figures 2 and 3 show a closer view of the radial fracture in the washer from the concave and convex sides, respectively. The opposite-facing fracture surfaces appeared rough and exhibited geometrical tortuosity. The washer was sectioned approximately 0.5 inches from one of the mating fracture surfaces. After cleaning in

an ultrasonic bath with acetone, the fracture surface could be examined, as demonstrated in Figure 4.

In a closer view in Figure 5, the washer exhibited woody or layered fibrous fracture features, consistent with a specific grain orientation and texture. The fracture surface was examined using a field emission scanning electron microscope (SEM). A typical area of the fracture surface near an edge on the concave side is shown in Figure 6. This figure demonstrates the elongated grain flow structure of the washer, oriented parallel to the washer's longitudinal direction (or perpendicular to the fracture surface).

The fracture surface exhibited a faceted fracture surface, as illustrated in Figure 6. This texture was consistent with fracture between some grains and cleaving along planes of others, consistent with mixed cleavage and intergranular fracture. Figure 7 shows the grain facets and tear ridges of several grains on the fracture.

A corner of the fracture surface of the washer exhibited a more rough and fibrous surface morphology (Figure 8). This area exhibited a 45° slant, consistent with a shear lip. A closer view of this area revealed dimpled rupture, as illustrated in Figure 9. The dimpled rupture on the corner, and the cleavage fracture over the rest of the surface, were consistent with the washer having fractured from overstress. Figure 9 shows a bent curving direction to the grain orientation along a corner (opposite the shear lip with dimpled rupture). This indicated the washer had been subjected to bending stresses.

The chemical composition of the washer was examined using energy dispersive x-ray spectroscopy (EDS). The chemical composition was consistent with high-strength steel. The hardness, examined per ASTM E18, averaged 48 HRC.[1,2] The fracture features were consistent with a material exhibiting this composition and hardness.

Figure 10 shows the lockwire, as received. The wire was approximately 1.99 inches long, with a wire diameter measured 0.024 inches. On the left of Figure 10, one end shows a small ovoid loop. The end on the opposite right side had been separated.

Figure 12 shows the fractured ends of the wires, constituting four fractured ends in total. The fractured ends each exhibited areas of smoothing, with a rougher center area. When examined using an SEM, the fractured ends in Figure 13 showed inward material deformation and smearing, followed by a rough texture and an outward protruding lip on the opposite side. The fourth wire, shown in Figure 14, exhibited opposite-facing V-shaped tears perpendicular to the fracture surface. There was also

[1] ASTM E18 – *Standard Test Methods for Rockwell Hardness and Rockwell Superficial Hardness of Metallic Materials*. ASTM International, West Conshohocken, PA.
[2] HRC – Hardness, Rockwell C scale. An indentation method of determining the hardness of harder metal alloys using a conical diamond indenter and 150 kg major load.

a second parallel notch below the fracture, which revealed streaks consistent with the smearing present on the fracture surface. The rough regions exhibited dimpled rupture, as shown in Figure 15. These features were consistent with the wire having been cut.

The loop of the lockwire was examined for witness marks that could indicate contact or wear against adjacent faying metal surfaces. Figure 16 shows a closer view of the wire loop, shown on the opposite side of Figure 10. This loop surface exhibited three marks containing an area of parallel rubbing or sliding lines, all located along the same side shown in Figure 16.

The distances between these witness marks were measured using a digital microscope, as annotated on the loop in Figure 17. The nearest distance between each of the pairs was 0.085 inches. The farthest distance of markings from the top and bottom of the loop was 0.146 inches.

An exemplar cap from the same assembly (but not the exact location of the cut lockwire in this case) was examined, as shown in Figure 18. The cap material was consistent with blue-anodized aluminum material. The cap was hexagonal, with three sets of holes at corners for wires to be positioned. One of the holes exhibited wear and enlargement, shown in Figure 19. The minimum distance between this hole was found to be 0.083 inches when measured with digital calipers and optical microscopy (see Figure 20). The other two holes exhibited lengths of 0.148 and 0.173 inches.

The two prominent witness marks on the lockwire were examined using an SEM, as shown in Figures 21 and 22. The backscattered micrographs show dissimilar material on the contact areas.[3] However, most of this material was found to be consistent with exogenous contamination (such as from oils or soil).

Some of the areas exhibited an area of dissimilar materials. One is highlighted in Figure 23. This area exhibited high levels of nickel and phosphorus, as shown in Figure 24. Another area exhibited small particles with high atomic number contrast (Figure 25). These particles were found to be consistent with tungsten (Figure 26). No areas exhibited dissimilar material consistent with aluminum or an aluminum alloy along the lock wire witness marks.

The worn holes of the cap were examined using EDS. Little of the surface area yielded conclusive EDS data, most of which was consistent with an aluminum alloy. Much of the surface was contaminated with elements such as Ca, Na, K, S, and Cl. However,

[3] Backscattered electrons – SEM micrographs produced using backscattered electrons display contrast that is associated with the atomic numbers of the elements in the micrograph. Materials containing elements with higher atomic numbers visually appear lighter relative to other materials containing elements with lower atomic numbers.

two areas inside one of the holes exhibited areas of dissimilar material. Each of these holes exhibited elevated levels of iron, as well as copper.

Submitted by:

Erik M. Mueller
Materials Research Engineer

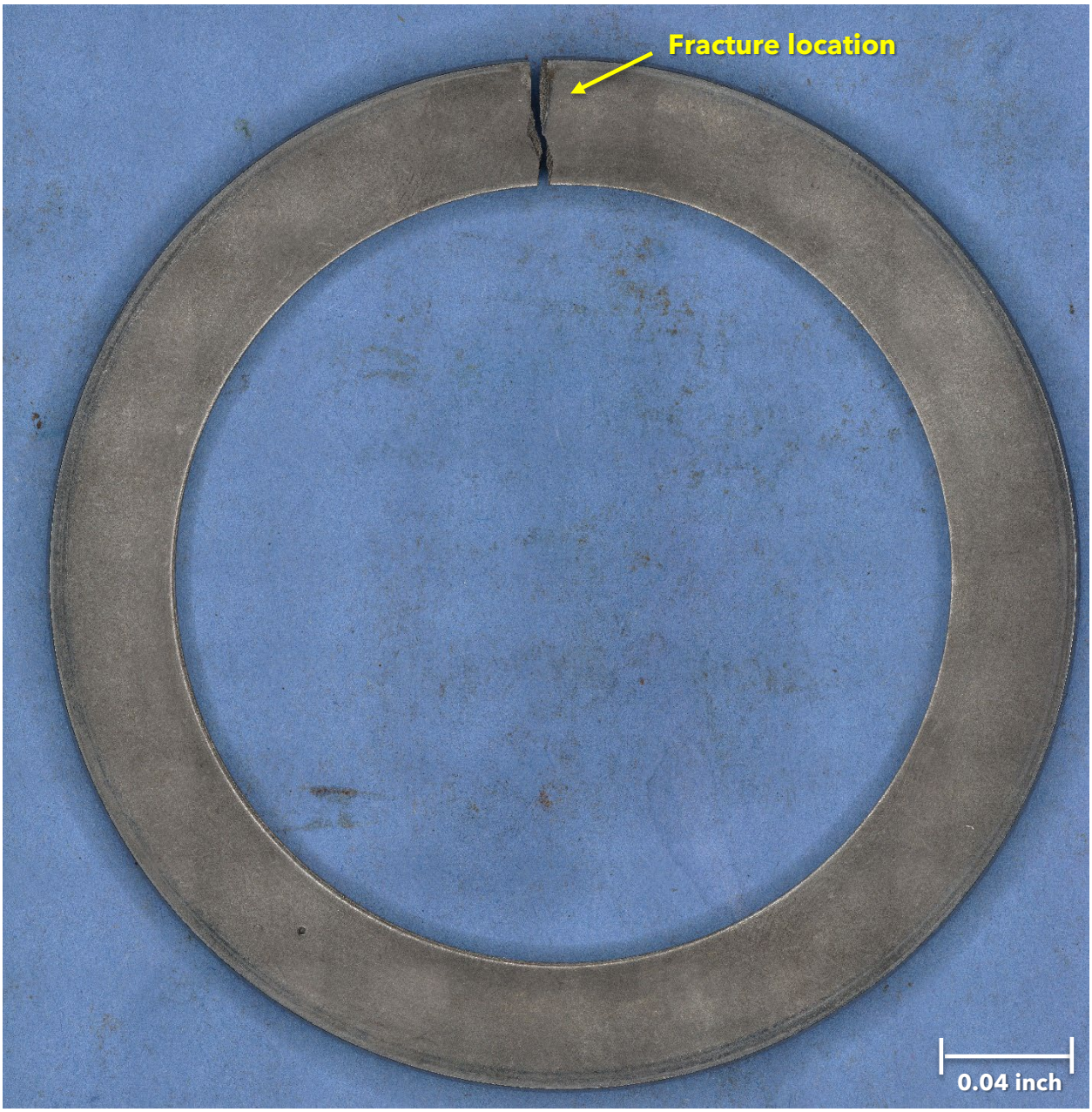

Figure 1. View of the washer from the concave side, as received, with the radial fracture shown in the 12 o'clock position.

Figure 2. Closer view of the fractured area of the washer from Figure 1, as received.

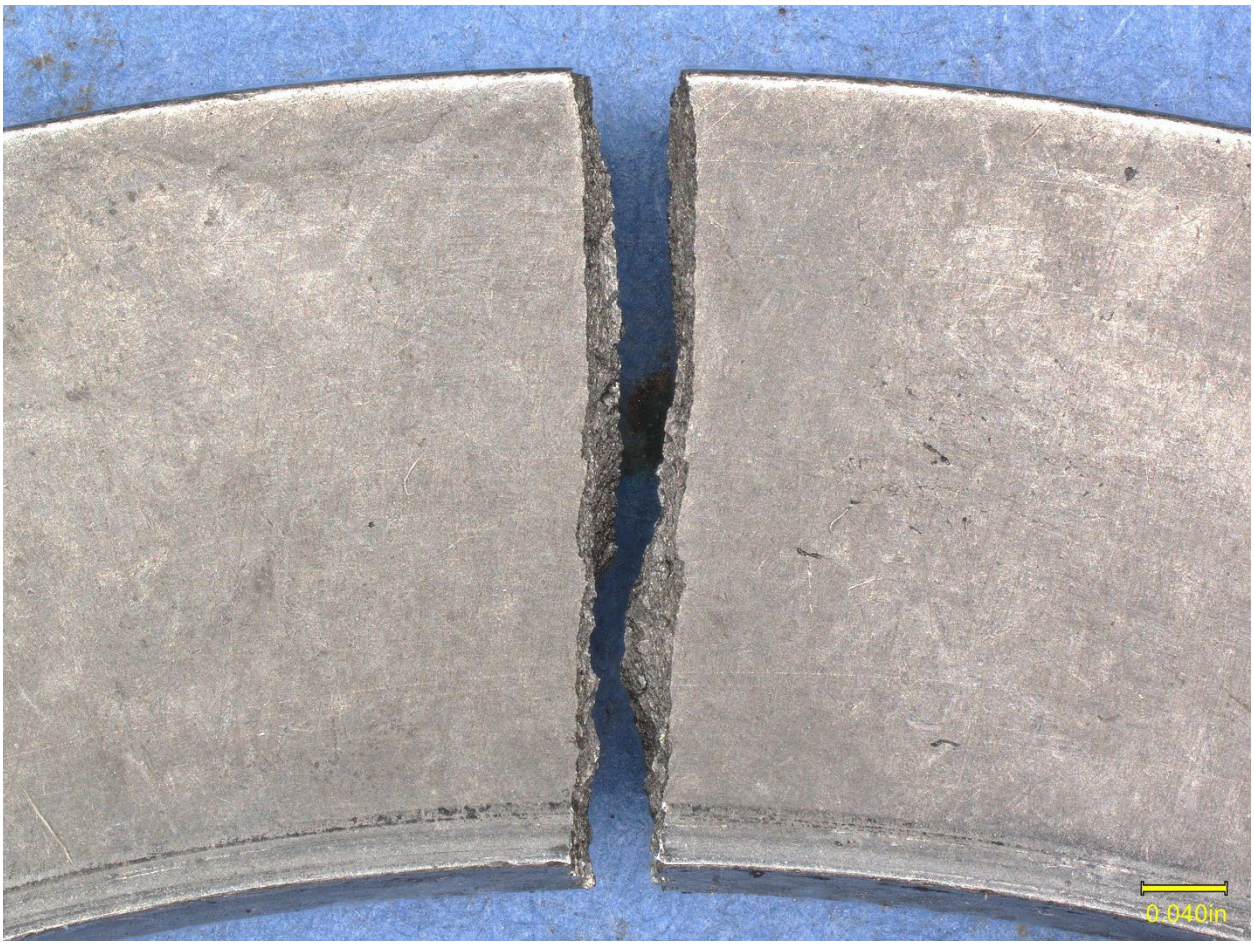

Figure 3. View of the fractured washer area from the opposite convex side, as received.

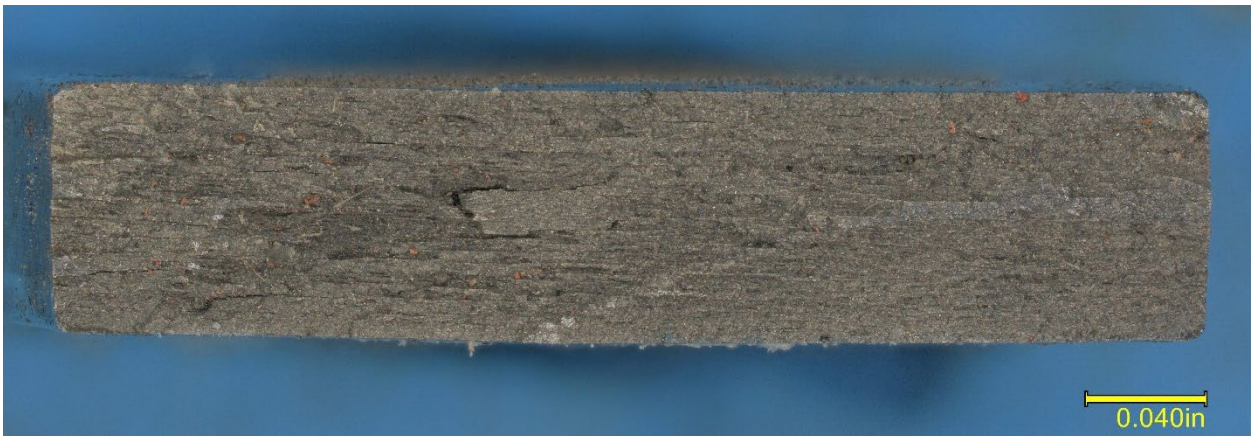

Figure 4. Overall view of the washer fracture surface, after sectioning.

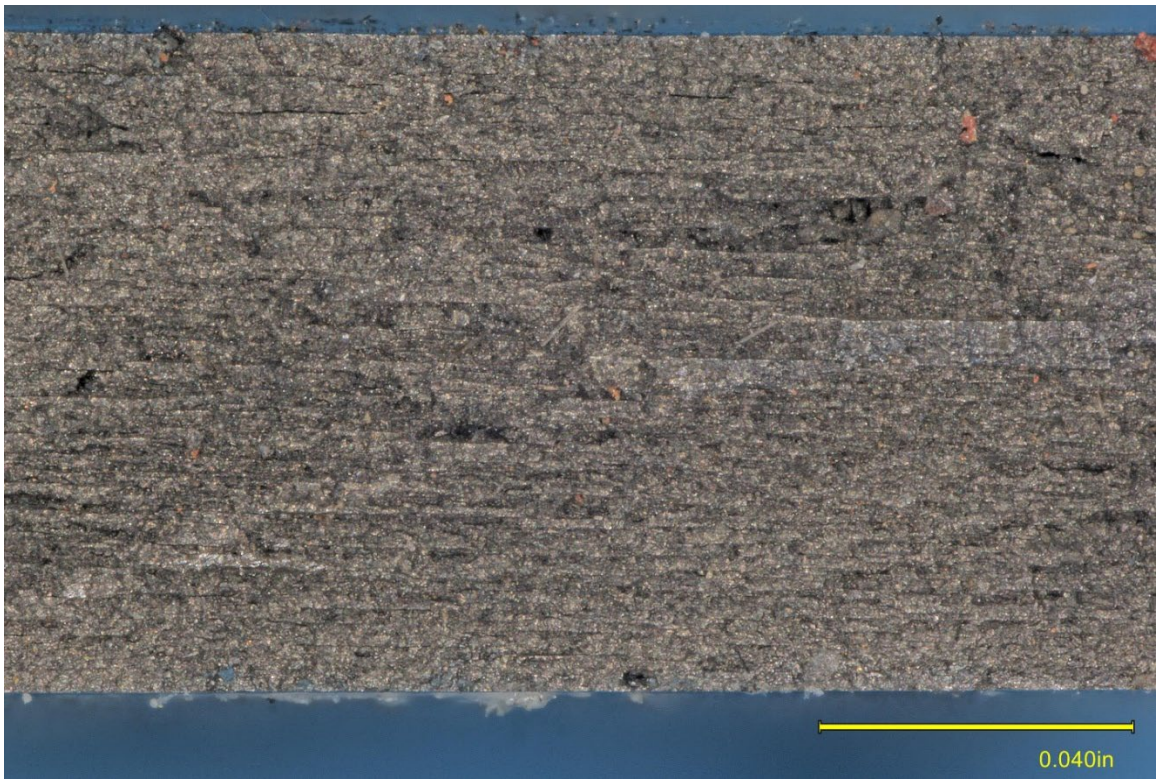

Figure 5. Closer view of the washer fracture, showing woody or fibrous fracture features.

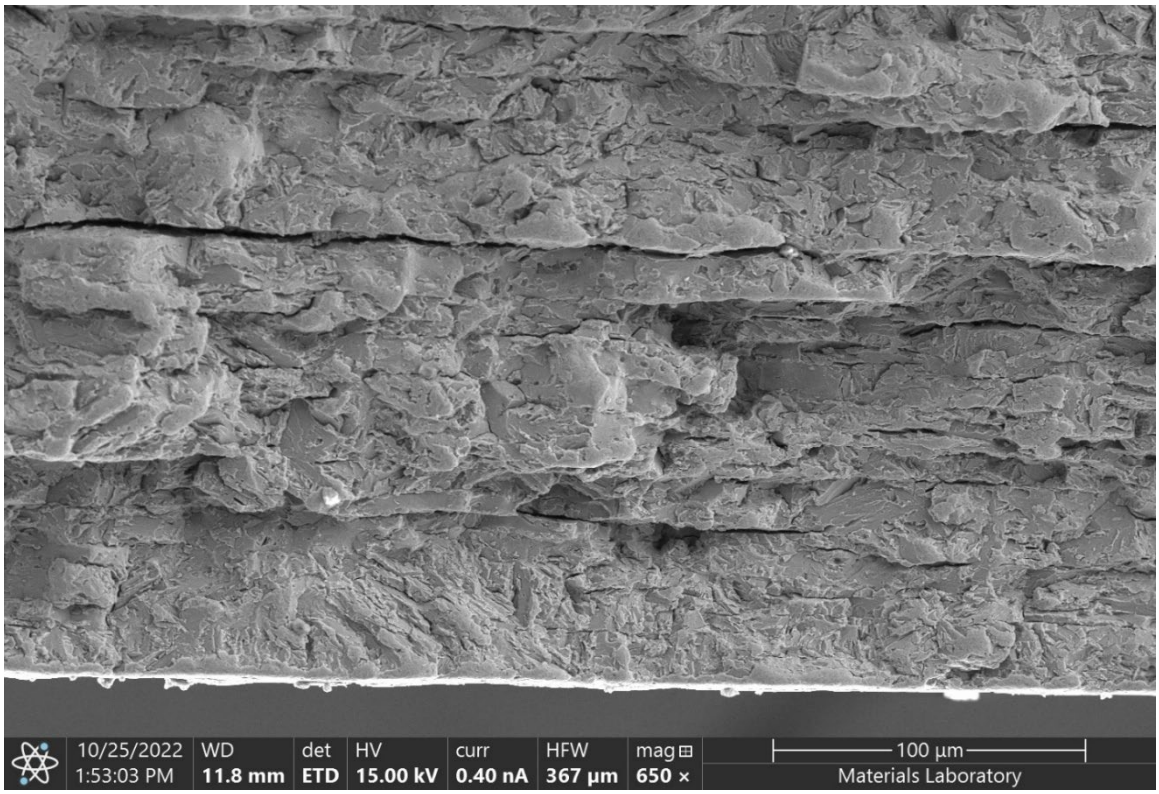

Figure 6. Secondary electron (SE) micrograph of the washer fracture surface, showing layered, fibrous features.

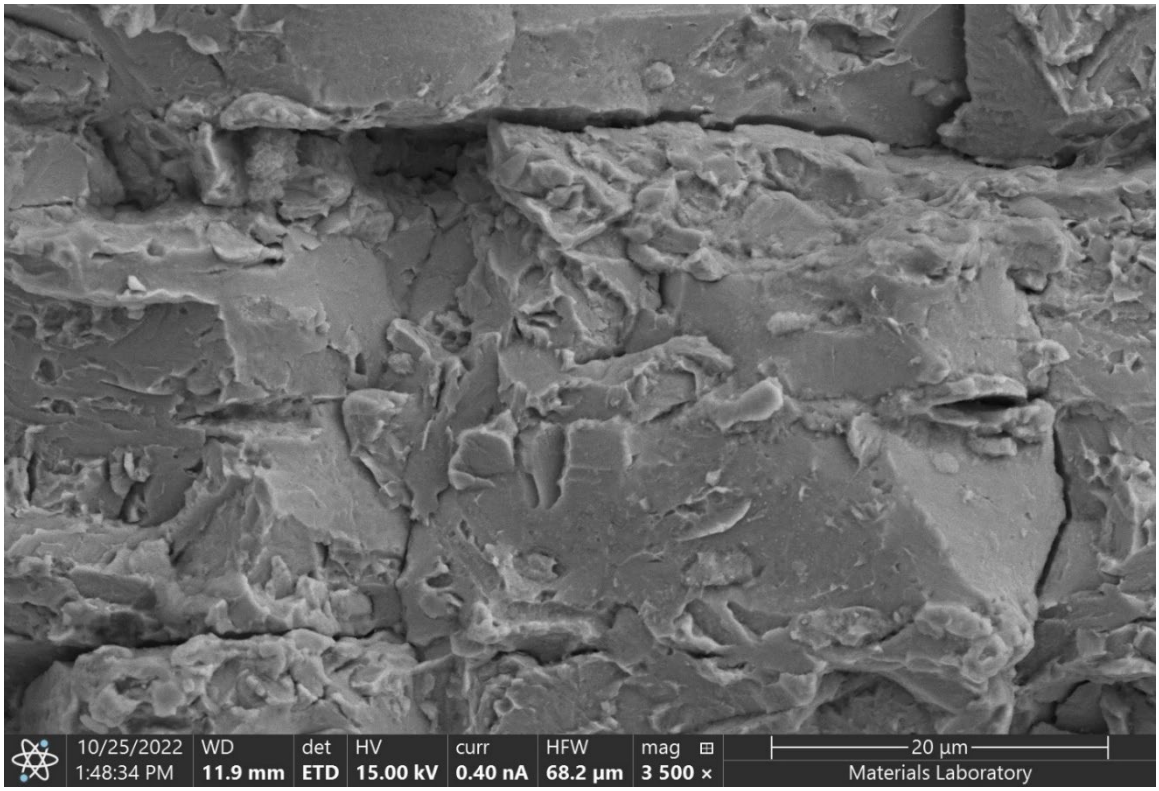

Figure 7. SE micrograph of cleavage facets and tear ridges on the washer fracture.

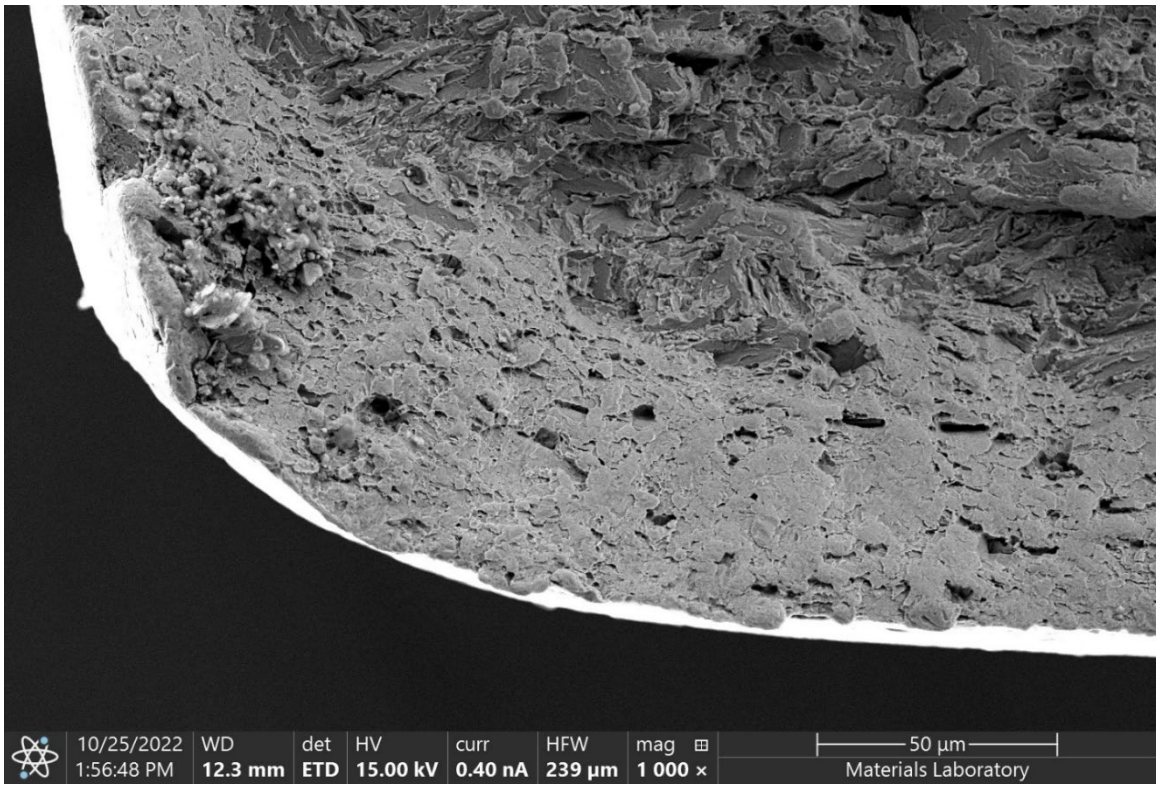

Figure 8. SE micrograph of a corner of the fracture surface, exhibiting a shear lip.

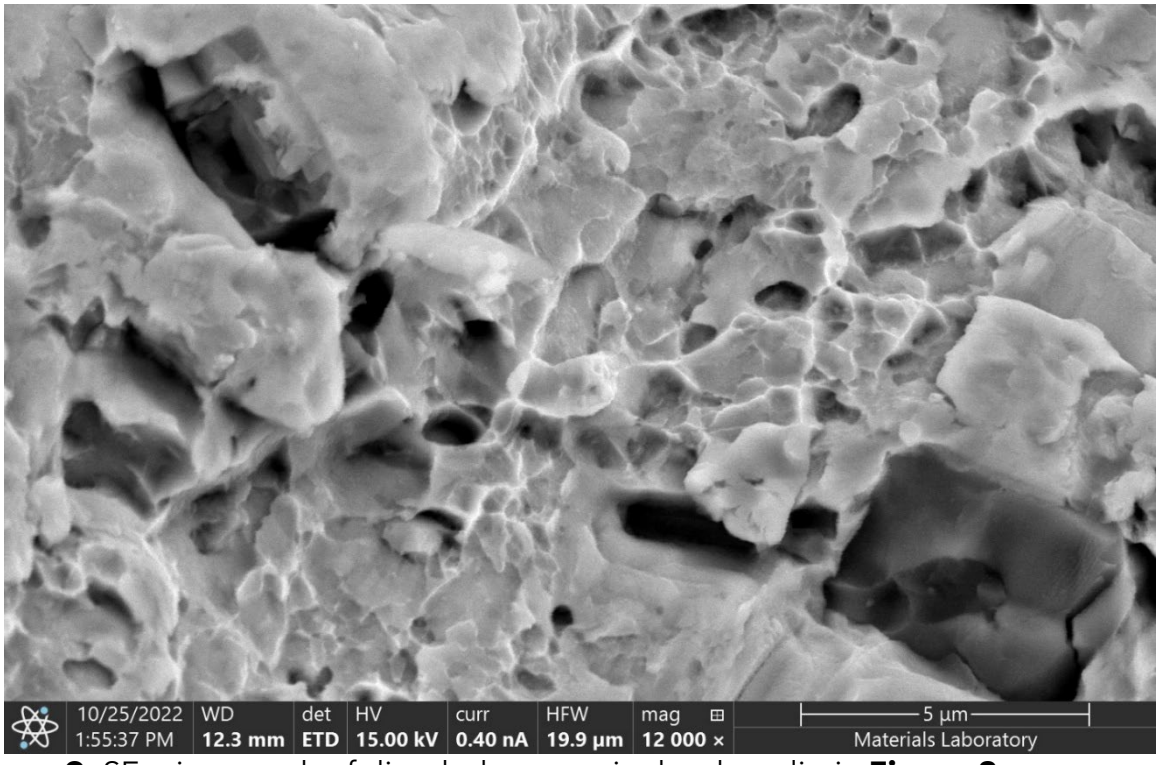

Figure 9. SE micrograph of dimpled rupture in the shear lip in **Figure 8**.

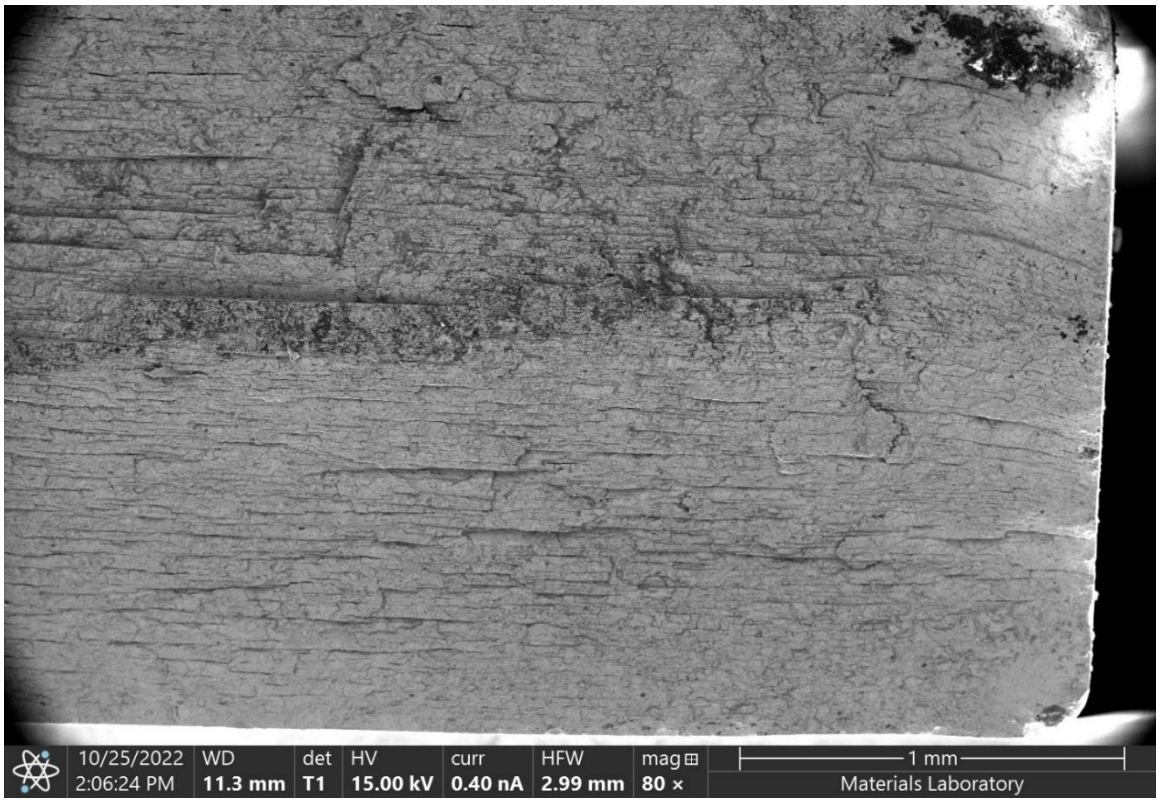

Figure 10. SE micrograph of deformation in the fractured grain structure on a side of the fracture surface of the washer.

Figure 11. Montage image of the lock wire section, as received.

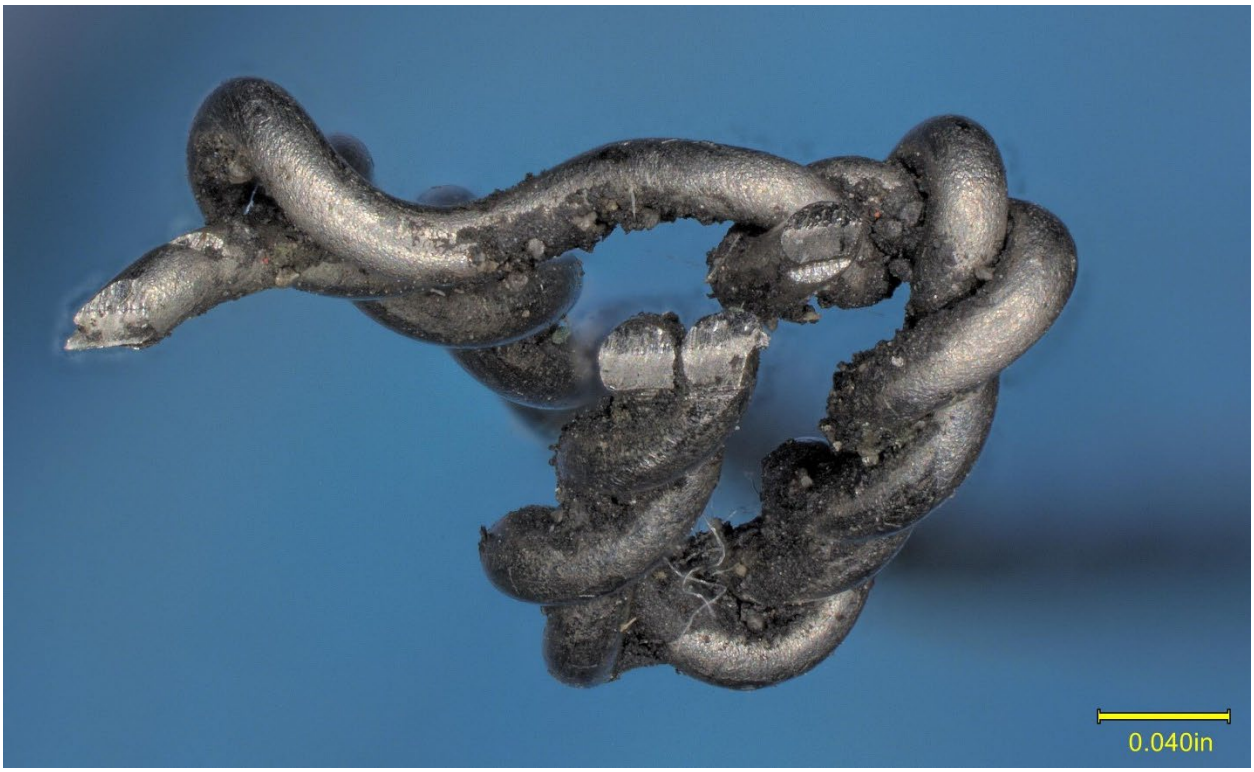

Figure 12. View of the fractured wires in the lock wire, as received.

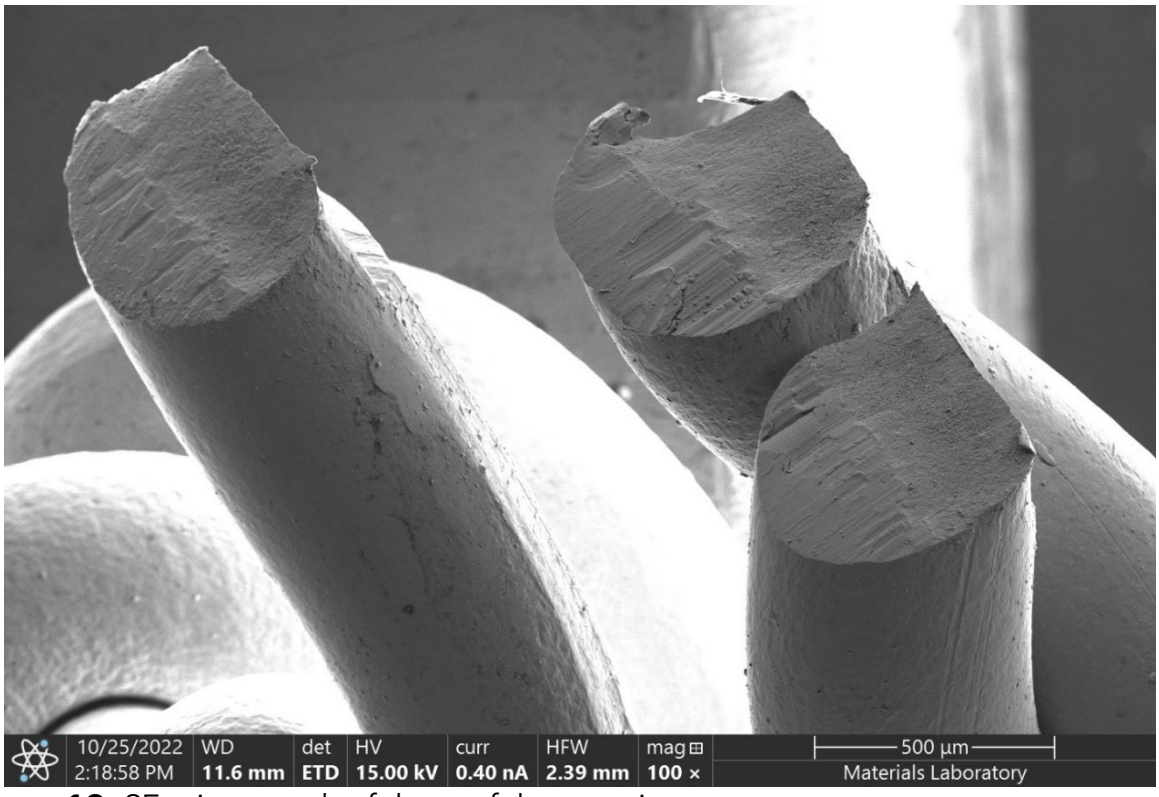

Figure 13. SE micrograph of three of the cut wires.

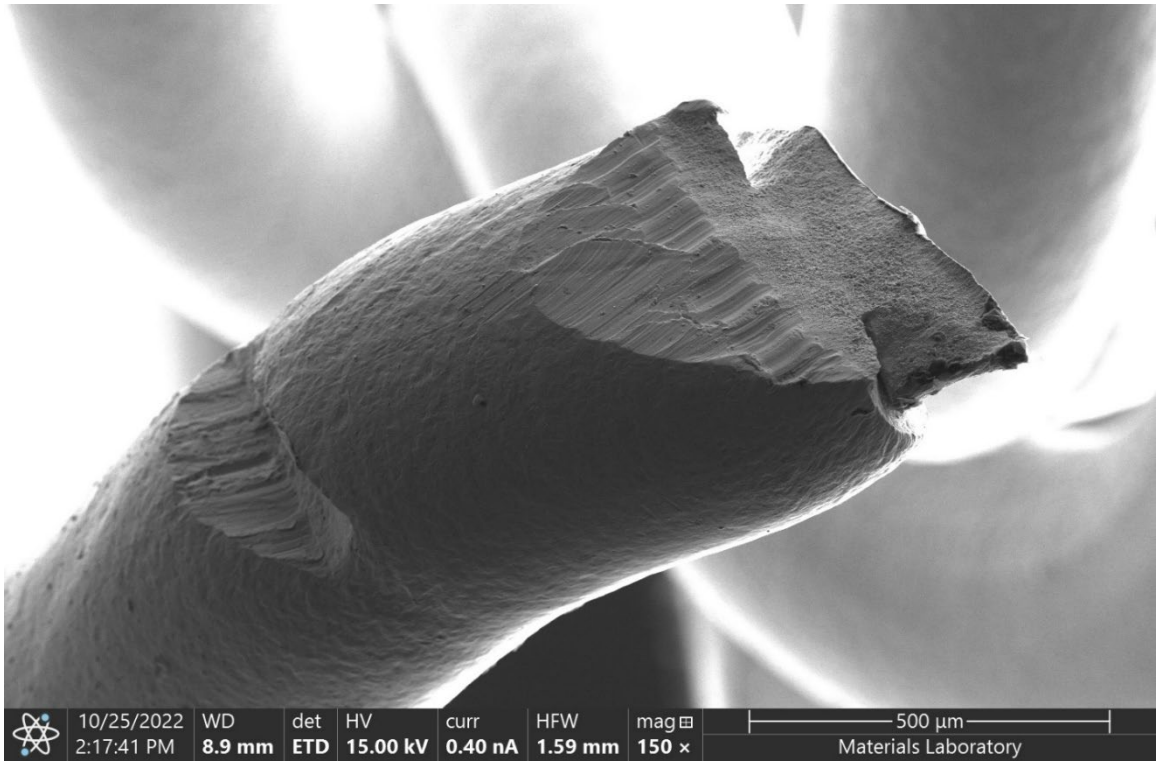

Figure 14. The fourth cut wire fracture surface, showing areas of smearing, pinching, and overstress.

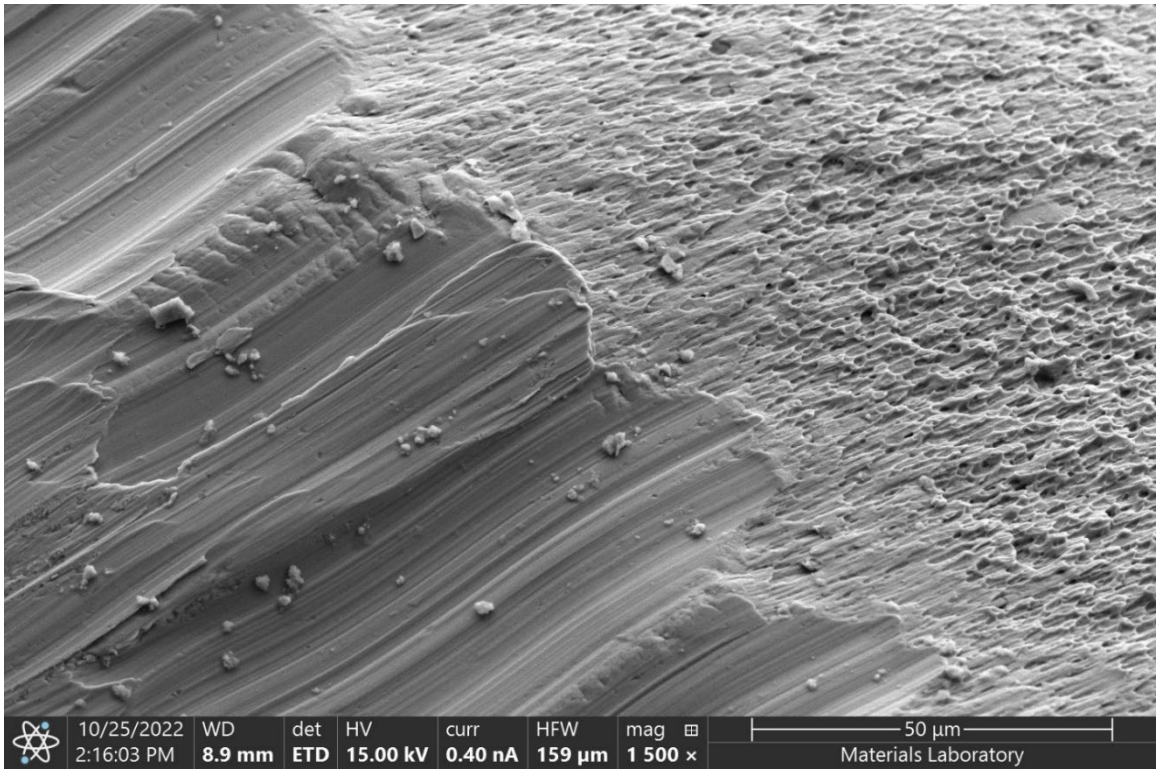

Figure 15. SE micrograph of shear dimpled rupture at the edge of the wire cutting.

Figure 16. Closer view of the loop of the lock wire, showing witness marks (arrows).

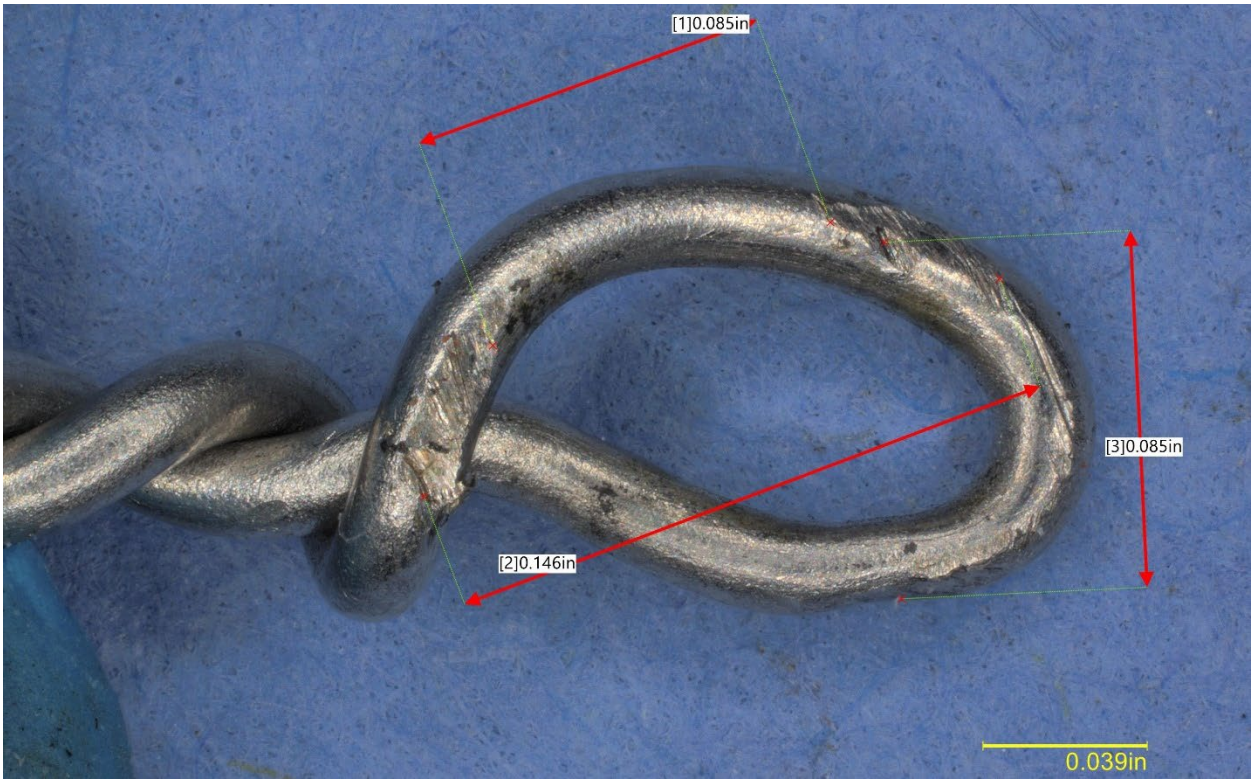

Figure 17. The lock wire loop in Figure 16, with various measurements annotated.

Figure 18. Side of the exemplar cap from an area of slight wear in the wire holes.

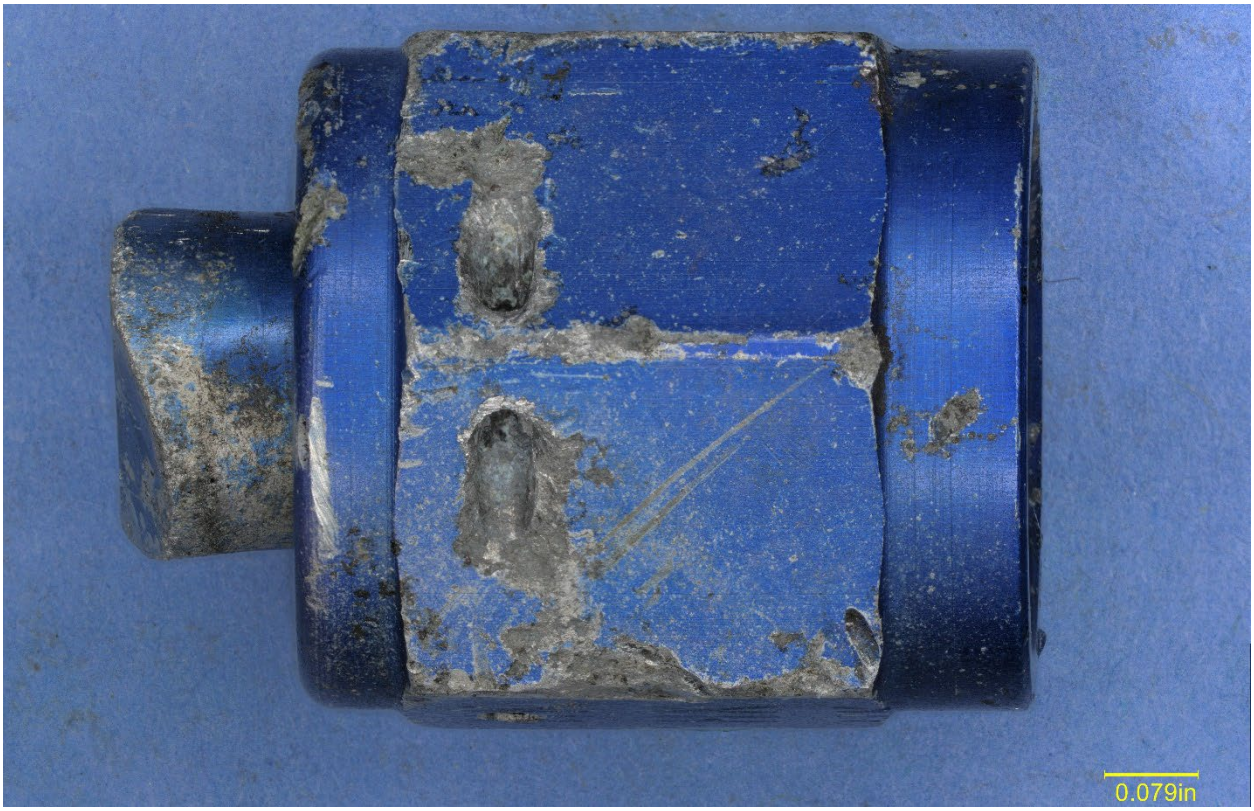

Figure 19. View of the worn wire holes of an exemplar cap from the same assembly.

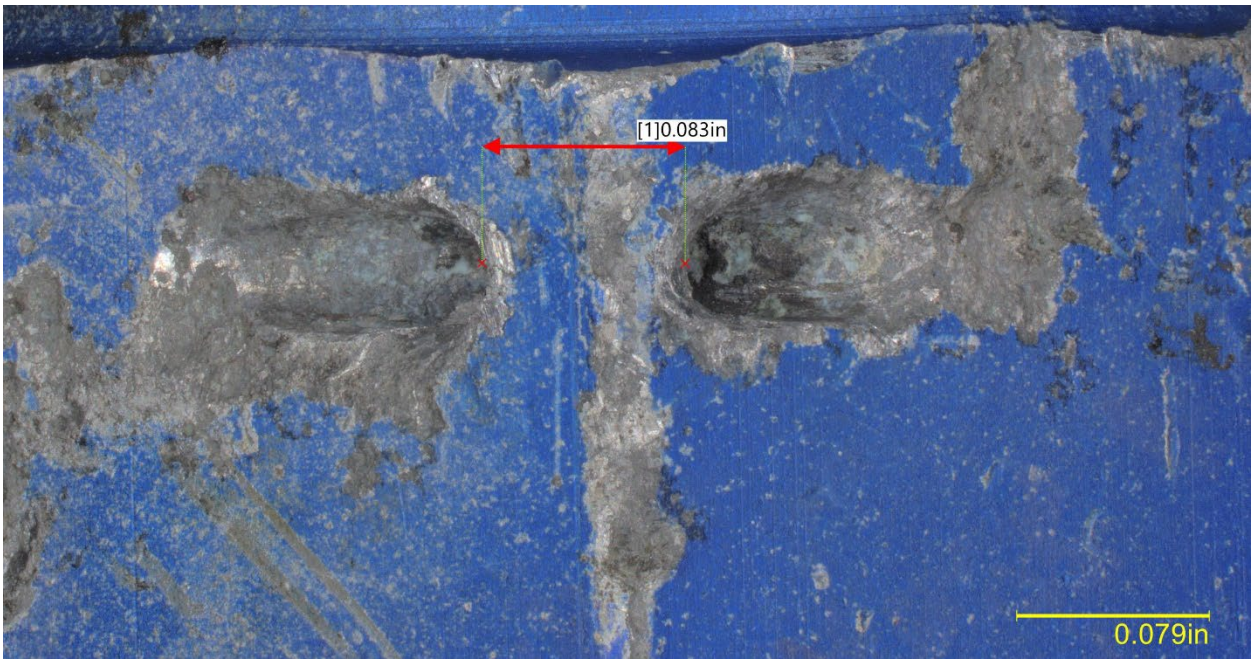

Figure 20. Measurement of the minimum distance between the worn wire holes of the cap.

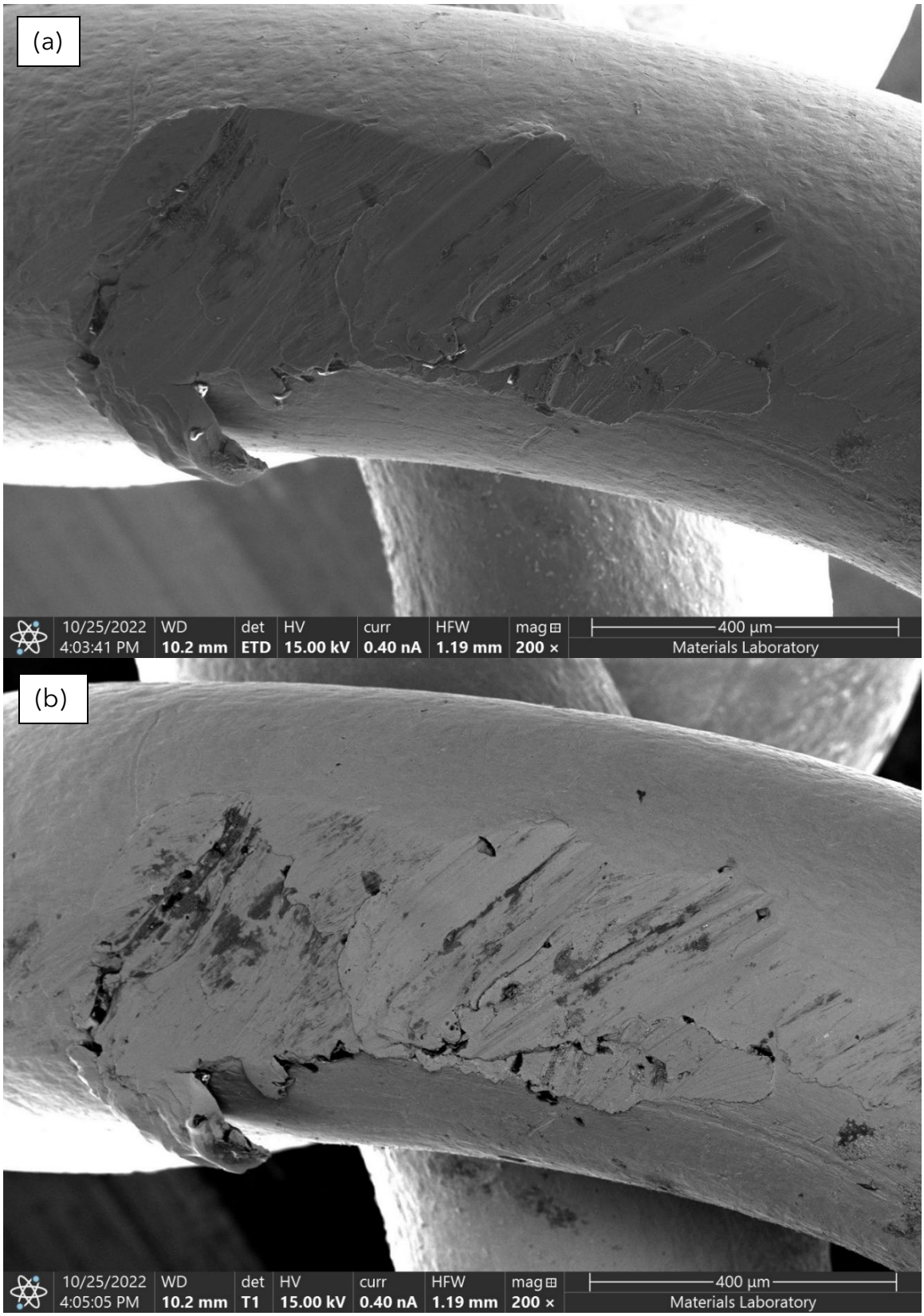

Figure 21. SE and backscattered electron (BE) micrographs of one of the witness marks on the loop of the lockwire.

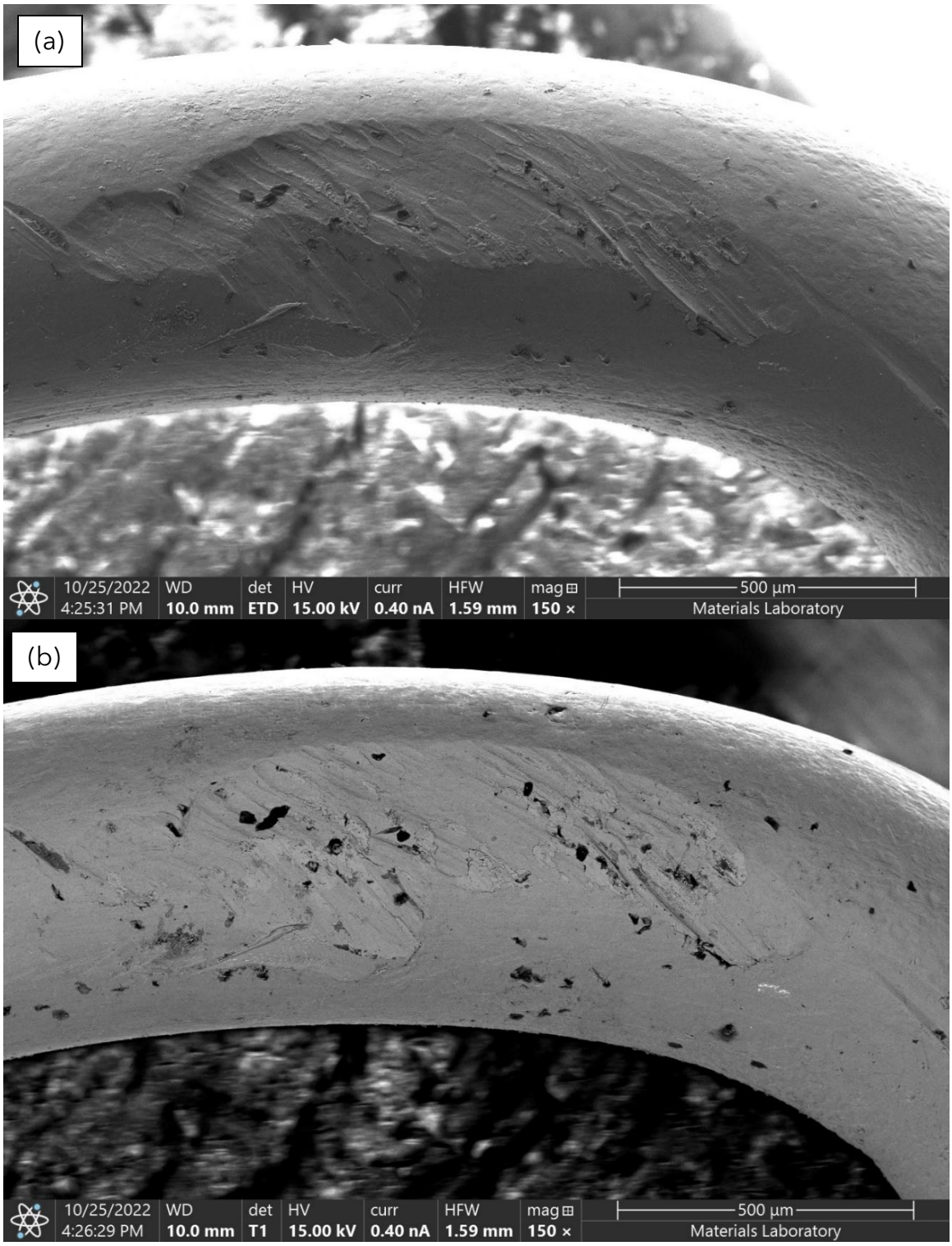

Figure 22. SE and BE micrographs of the second witness mark on the loop of the lockwire.

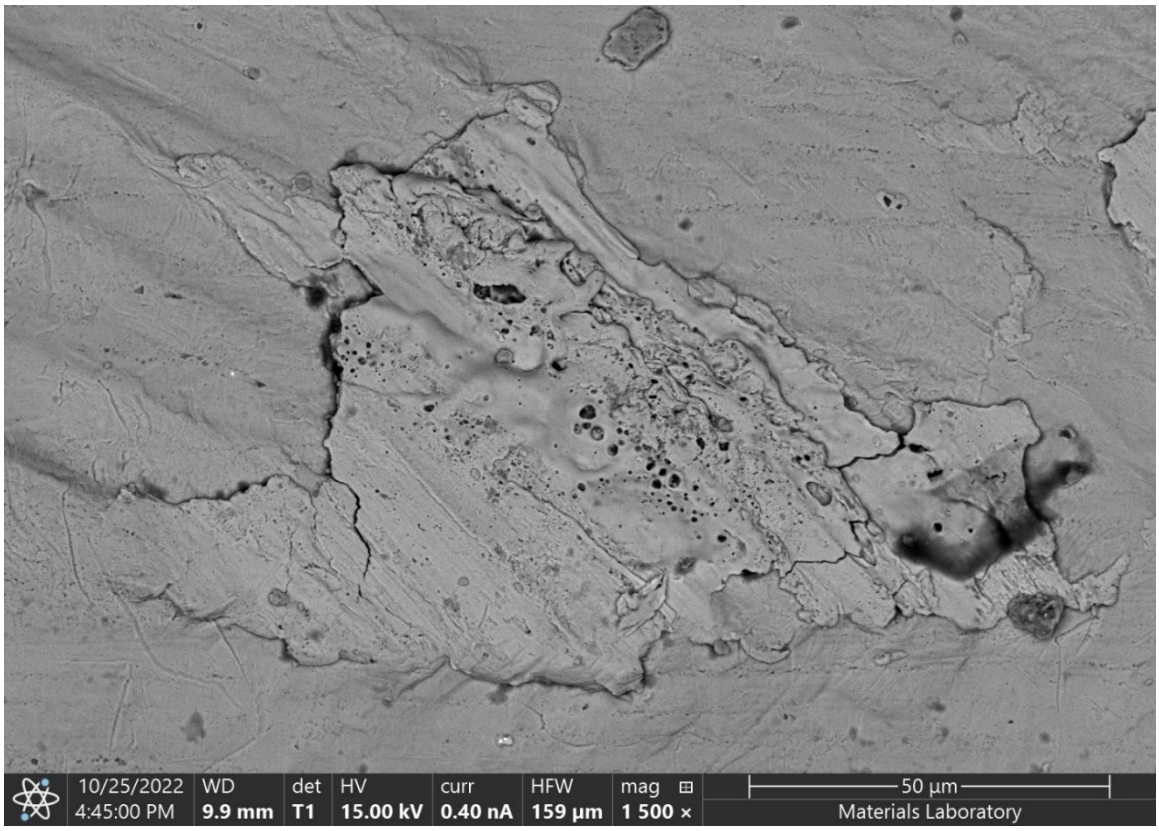

Figure 23. BE micrograph of a deposit on the witness mark in **Figure 22**, showing an area high in nickel and phosphorus.

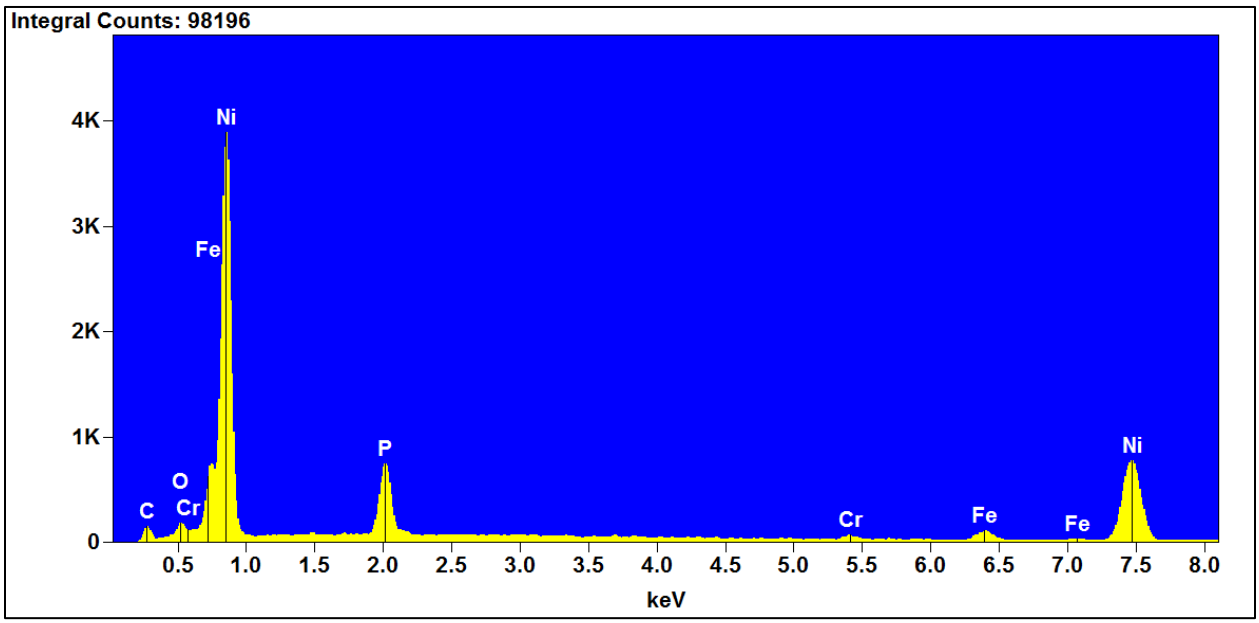

Figure 24. EDS spectrum of the area in **Figure 23**, showing high amounts of nickel and phosphorus.

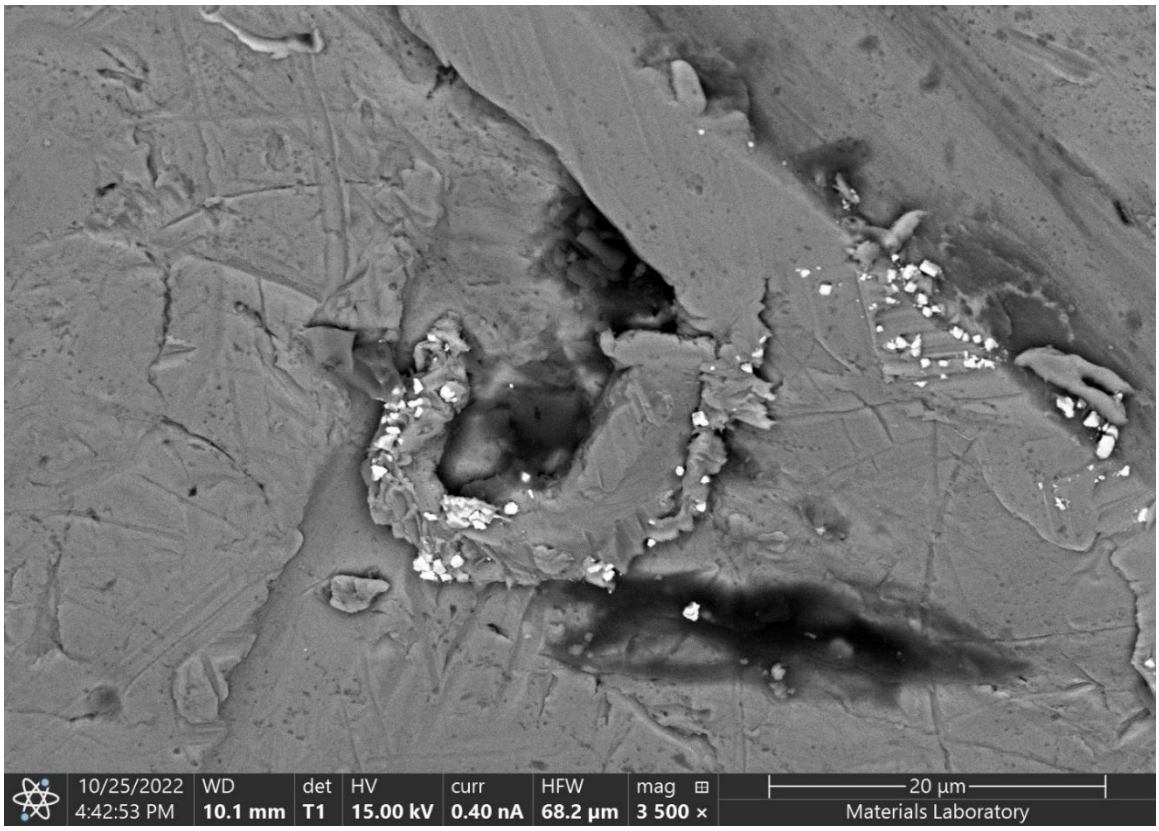

Figure 25. BE micrograph of a small, high atomic number materials on the witness mark in **Figure 22**, showing high tungsten content (see **Figure 26**).

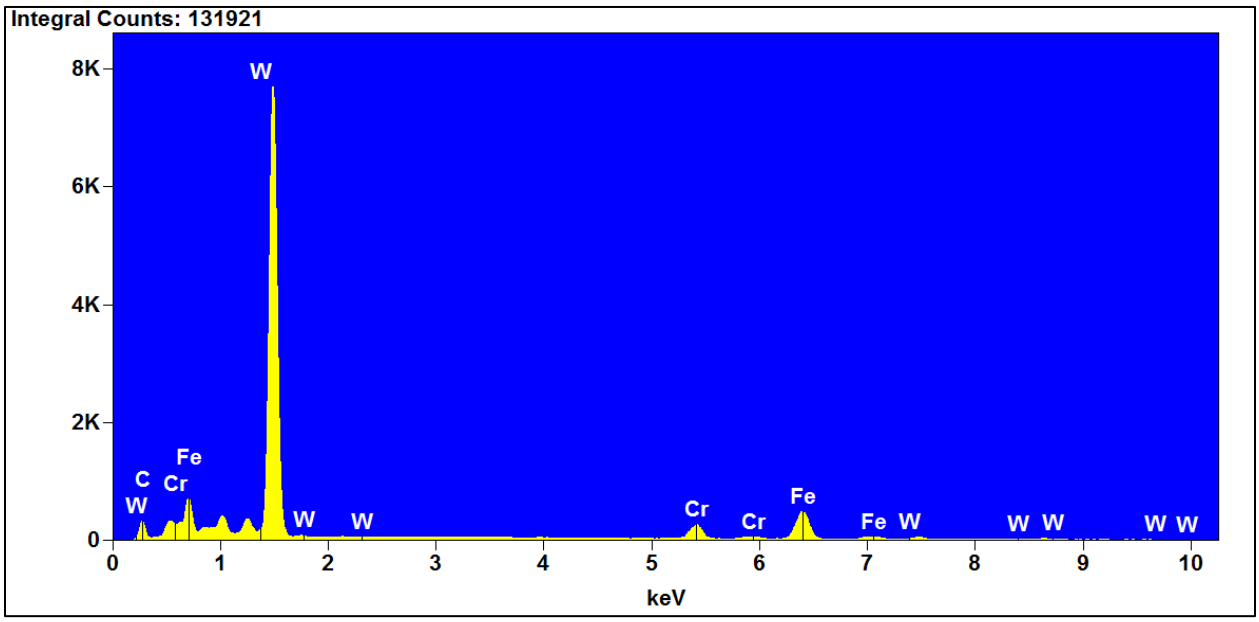

Figure 26. EDS spectrum of the white areas in **Figure 25**, showing mostly tungsten (W).